Visible-infrared spectroscopy and chemical properties of water in mining area

Aliyeh Seifi, Mahdieh Hosseinjanizadeh, Hojjatolah Ranjbar and Mehdi Honarmand

ABSTRACT

The present research focuses on investigating the relationship between spectral and chemical characteristics of water samples in Darrehzar mine. In order to reach this aim, the chemical characteristics of water were measured through pH, electrical conductivity (EC) and inductively coupled plasma mass spectrometry (ICP-MS) analysis. Furthermore, the visible near infrared (VNIR) and shortwave infrared (SWIR) spectra of water samples were measured by Analytical Spectral Devices (ASD) FieldSpec[3] spectroradiometer and the relationships between spectral and chemical characteristics of water samples were calculated. Results of the pH and EC measurements showed that water with high acidity and EC values, which indicate the presence of acid drainage, was located inside the mine. High concentrations of copper, sulfur and iron in the samples could be related to copper mineralization and association with acid mine drainage. Results of spectroscopy revealed that second absorption feature (AF2) magnitude correlated significantly with pH (-0.599), EC (0.611) ($p < 0.1$) and total trace elements plus sulfur (0.822) ($p < 0.05$). The significant correlation of the AF2 magnitude with concentrations of S (0.854), Pb (0.914), Ni (0.836), Mn (0.834), Co (0.848) and AF3 with the concentration of Fe (0.886) confirms that absorption feature magnitude increases with increasing metals concentrations in water.

Key words | absorption feature, chemical characteristics of water, Darrehzar mine, field spectroscopy, pH and EC

Aliyeh Seifi
Mahdieh Hosseinjanizadeh (corresponding author)
Mehdi Honarmand
Department of Ecology, Institute of Science and High Technology and Environmental Sciences, Graduate University of Advanced Technology, Kerman, Iran
E-mail: *m.hosseinjanizadeh@kgut.ac.ir*

Hojjatolah Ranjbar
Department of Mining Engineering, Shahid Bahonar University, Kerman, Iran

INTRODUCTION

Water is a strongly reactive material which can dissolve elements and objects when it moves through porous media. The solubility of minerals increases in mining areas due to the fractures. Fractured surfaces provide more exposed surface and that, in turn, causes more chemical reactions between the water and the minerals. In sulphidic mines, oxidation and dissolution of sulphide minerals such as pyrite, chalcopyrite and sphalerite raises the hydrogen and sulphates in the water. As a result, water acidification occurs, water acidity increases and pH of water reduces (Blahwar 2010; Gyuris *et al.* 2010). Acidic water enables the

dissolution of heavy metals so that with the rise in acidity, the sulphates and metals concentrations will be increased in the water.

An assessment of acidity values and environmental degradation was carried out in the Witwatersrand basin (South Africa) and Caveira abandoned mine (Southern Portugal) through temperature, H^+ activity (pH), oxidation-reduction potential (Eh), electrical conductivity (EC), inductively coupled plasma (ICP) and ion chromatography (IC) measurements (Tutu *et al.* 2008; Ferreira da Silva *et al.* 2015). Furthermore, geochemical studies were performed in the stream water, stream soil and stream sediments of Darrehzar mine, Iran, using pH, Eh, EC, atomic absorption spectroscopy (AAS) and inductively coupled plasma mass spectrometry (ICP-MS) in order to identify acid mine drainage pollution and determine trace metals and rare earth elements (Moor *et al.* 2012; Soltani *et al.* 2014).

Spectroscopy, which is one of the applicable methods in identification of ground materials, benefits from different parts of the electromagnetic (EM) spectrum in material detection (van der Meer & de Jong 2006). Since water plays an important role in nature, water spectroscopy studies should be a priority in research (Yamanouchi & Tanaka 1985; Buiteveld *et al.* 1994). A number of water studies focus on laboratory and mathematical studies for determining the relationship between spectral absorption of water with temperature and salt dependencies in the ultraviolet, visible and infrared portions of the EM spectrum (Sullivan *et al.* 2006; Wang 2008).

The spectral studies in the mining areas related to acid mine drainage (AMD) have been focused on reflectance spectral characterization of iron-oxide and sulphate minerals through field spectrometry and hyperspectral data (Anderson & Robbins 1998; Shi *et al.* 2014). In addition, some studies focused on investigation of heavy metal concentration in deposits and vegetations of mining areas (Choe *et al.* 2008; Li *et al.* 2008; Khalili *et al.* 2015). Mapping of heavy metal pollution in stream sediments using field spectroscopy revealed that variations in the spectral absorption features were linked to actual concentrations of heavy metals. So that, heavy metals concentrations in minerals increase the depth of absorption features in the visible part (around 500 nm) and decrease the absorption depth in the shortwave infrared (SWIR) region (around 2,200 nm, where it is related to the OH bound in minerals) (Choe *et al.* 2008). Heavy metals accumulation in vegetation can also cause some effects such as an increase in the spectral reflectance, the occurrence of spectral shape blue-shift, increase in the red edge slope, decrease in the chlorophyll

and water absorption depth, occurrence of the water absorption red-shift and change in the spectral profiles in the visible and near infrared portions (Li *et al.* 2008; Khalili *et al.* 2015).

Although spectral studies have been carried out for determination of the relationship between water absorption features with temperature and salinity of water as well as heavy metal levels in minerals and vegetation, the influence of heavy metals and pH in the spectral properties of water in mining areas has not been investigated yet. While increasing heavy metals can cause environmental pollutants and affect human health, applying these kinds of studies could be significant. Hence, in the present study, the chemical properties of water in Darrehzar mine, such as trace elements plus sulfur concentrations, pH and EC as well as spectral features of water samples, were measured in order to investigate the relationship between the spectral characteristics in the visible-infrared portion and the chemical composition of the water.

Study area

Darrehzar porphyry copper mine is located about 10 km south of the well-known Sarcheshmeh porphyry copper mine in Kerman province, south east of Iran (Figure 1). The area has a moderate climate, with a temperature range between $-15\,^{\circ}C$ (winter) and $+33\,^{\circ}C$ (summer), and annual precipitation from 300 to 500 mm. Darrehzar river, with N-S direction, intersected the mine into west and east parts. The river was permanent in the past with a discharge rate of about 7 m^3/s at the end of winter and in the first days of spring. However, as a result of recent droughts, this river
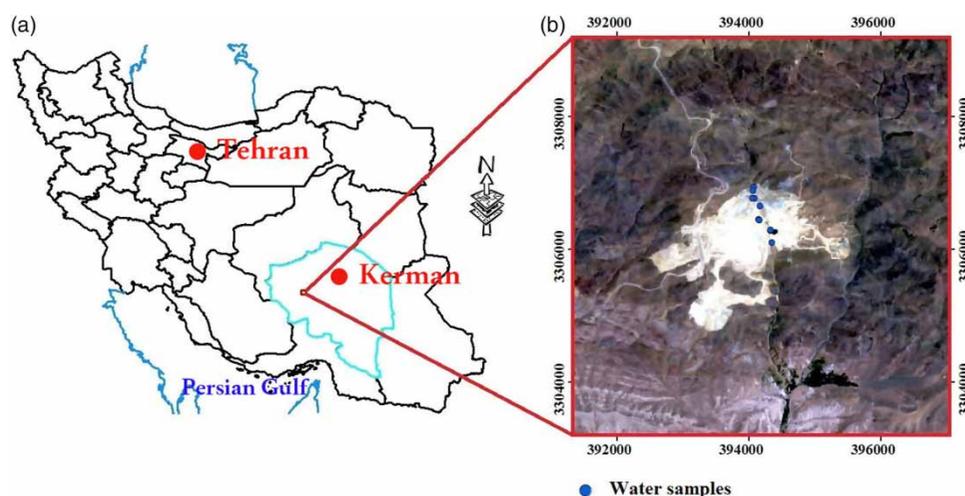

Figure 1 | (a) Location of the study area in Iran and Kerman province; (b) location of water samples, which were plotted on Sentinel 2a image (acquisition time: 18 July, 2016).

is not permanent and only in the wet seasons (winter and spring) is observed in the area (GSI 1973; Soltani et al. 2014).

The lithology of the area consists of Oligocene-Miocene dioritic and quartz dioritic bodies which were intruded into Eocene volcanic rocks composed mainly of volcanoclastics, andesite and trachyandesite rocks. Sericitic, silicic, chloritic, argillic and locally biotitic alterations are developed both in the intrusive bodies and in their host rocks. Three main fault systems have been recognized with an E-W (pre-mineraliz-ation fault), a NW-SE (mineralized fault) and a N-S striking (post-mineralization fault) in the Darrehzar deposit (GSI 1973; Ranjbar et al. 2000; Nateghi & Hezarkhani 2013; Hosseinjani Zadeh et al. 2014).

MATERIALS AND METHODS

Since normally different metal concentrations were found in winter and summer seasons (Ferreira da Silva et al. 2015), water samples were collected from Darrehzar mine during two periods of field reconnaissance in the winter and summer of 2016 in the present research. Eight water samples were collected from different parts of the mine, including: influx water to the mine (sample from a surface water river named Da31), near influx water to the mine (sample from a surface water river named Da22, Da29 and Da 30), groundwater in a piezometer well in the mine (Da32), a surface water lake in the eastern part of the mine (Da23-1), a surface water pit lake in the western part of the mine (Da20-1), and discharging water from the mine (sample from surface water river named Da24) in the winter season (first field reconnaissance). However, in

the summer season (second field reconnaissance) influx and discharging waters of the mine had dried up and the water table in the piezometer well had fallen, so only two water samples were collected including the surface water lake in the eastern part of the mine (Da23-2) and the surface water pit lake in the western part of the mine (Da20-2) (Table 1). Two samples were taken from each sampling point simultaneously. One was collected for EC, pH and spectroscopy analysis and the other, which was acidified to pH < 2 with nitric acid (HNO_3), for measuring elements concentrations.

Water samples were collected in polyethylene bottles and their temperatures were recorded onsite. The collected water samples were transferred to Graduate University of Advanced Technology laboratory for EC, pH and spectroscopy measurements. The pH and EC of water samples were measured by Metrohm 827 laboratory pH meter and Metrohm 712 Conductometer EC meter. The spectroscopy analyses of the samples were conducted by ASD (Analytical Spectral Devices) FieldSpec$^{®3}$. Trace element concentrations of acidic water samples were determined by ICP-MS using an Agilent series 4500 instrument. These samples were gathered from different parts of the mine including the surface water lake in the eastern part of the mine (Da23-1 and Da 23-2), the surface water pit lake in the western part of the mine (Da20-1 and Da20-2), the influx surface water river to the mine (Da31) and the discharge surface water river from the mine (Da24). The elements' concentrations and pH values were compared with standard values of drinking and natural mineral waters. In order to compare EC with standard values, first EC was converted to total dissolved solids (TDS) by multiplying by an

Table 1 | The geographic locations of water samples

Sampling date	Sample number	Sampling site	Northing (UTM)	Easting (UTM)
08 March 2016	Da20-1	SWp in the western part of mine	3306444	394157
08 March 2016	Da22	SWr in the mine site	3306653	394170
08 March 2016	Da23-1	SWl in the eastern part of mine	3306288	394330
08 March 2016	Da24	SWr in the mine site (Downstream)	3306097	394347
08 March 2016	Da29	SWr in the mine site	3306773	394077
08 March 2016	Da30	SWr in the mine site	3306772	394051
08 March 2016	Da31	SWr in the mine site (Upstream)	3306942	394074
08 March 2016	Da32	GW (piezometer well) in the mine	3306885	394056
20 July 2016	Da23-2	SWl in the eastern part of mine	3306285	394327
20 July 2016	Da20-2	SWp in the western part of mine	3306453	394145

GW: groundwater, SWr: surface water river, SWl: surface water lake, SWp: surface water pit lake.

experimental coefficient (https://www.translatorscafe.com/unit-converter/en-US/electric-conductivity/) and then TDS values were evaluated to standard values.

Noises were removed from the spectra of water samples using ViewSpec Pro and SAMS (Spectral Analysis and Management System) software and the magnitude of absorption features in the spectra were analyzed with Equation (1) through SAMS software.

$$\alpha i = 1 - \frac{area\ under\ curve\ in\ [wp\ \&\ wq]}{area\ under\ line\ segment\ connecting\ si\ (wp)\ and\ si\ (wq)}$$
(1)

In this equation, αi is absorption feature analysis, si is absorption feature signature, wp is the wavelength of the maximum reflectance point before the absorption feature and wq is the wavelength of the maximum reflectance point after the absorption feature (Rueda & Wrona 2003).

The relationship between pH, EC and trace elements and sulfur concentrations (Al, As, Cd, Co, Cu, Fe, Mn, Mo, Ni, Pb, S, Sb and Zn) of water samples with absorption features analysis were determined through the regression coefficient (R) and the significance threshold value were defined at 0.01, 0.05 and 0.1. The flowchart of the study procedure is shown in Figure 2.

RESULTS AND DISCUSSION

Chemical properties

Results of chemical parameters of water samples showed that samples from the surface water lake in the eastern part of the mine (Da23-1 and Da23-2) and surface water pit lake in the western part of the mine (Da20-1 and Da20-2) are characterized by low pH and high EC. The reason could be attributed to the situation of these samples which correspond to the phyllic alteration zone. Actually, this zone contains more than 10% pyrite and pyrite oxidation generates acid mine drainage (Costello 2003; Moor *et al.* 2012). Comparison of these samples (Da23-1, Da23-2, Da20-1 and Da20-2) with the maximum contaminant level (MCL) for drinking water introduced by institute of standards and industrial research of Iran (ISIRI) revealed that the pH values of the samples were less than the pH of MCL; however, the TDS values were determined between the admissible limit (1,000 mg/l) and MCL (1,500 mg/l) (ISIRI 1053 2009). Moreover, pH levels of water in both places have reduced while EC and TDS have increased from winter to summer at these locations due to the heat and evaporation in summer which reduce the water content at the area. The TDS values of water
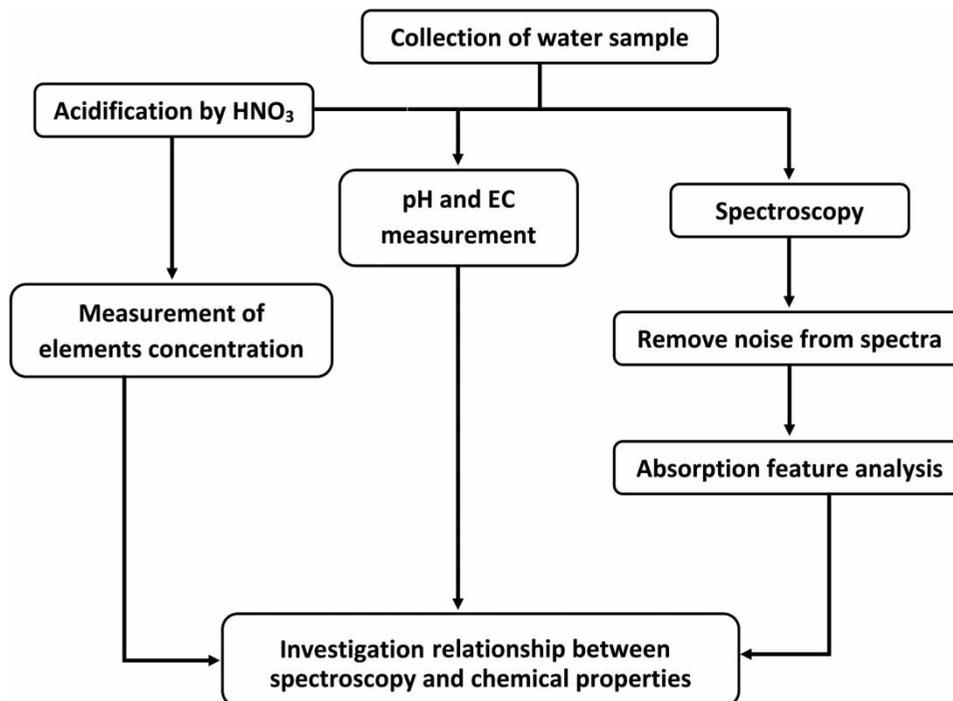

Figure 2 │ Flowchart of the study procedure.

samples from groundwater in piezometer well in the mine (Da32) and surface water river in the bottom of the piezometer well in the mine (Da30) were also between the admissible limit (1,000 mg/l) and MCL (1,500 mg/l) of standard TDS (ISIRI 1053 2009) (Table 2).

Table 2 │ pH, EC and TDS for the water samples

Sample name	pH	EC (μs/cm)	TDS (ppm)
MCL	6.5–9	–	1,500
Da20-1	3.48	1,570	1,004.8
Da22	8.09	484.4	310.016
Da23-1	4.28	1,583	1,013.12
Da24	7.88	582.5	372.8
Da29	6.6	645.8	413.312
Da30	7.43	1,948	1,246.72
Da31	7.9	453.7	290.368
Da32	7.23	1,991	1,274.24
Da23-2	3.18	2,218	1,419.52
Da20-2	2.75	2,247	1,438.08

MCL: maximum contaminant level.

In addition, elements such as; Al, As, Cd, Co, Cr, Cu, Fe, Mn, Mo, Ni, Pb, S, Sb and Zn were analyzed using ICP-MS. Result of ICP-MS shows that Al, Cu, Fe, Mn, S and Zn (mg/l) concentrations were higher than other elements (Figure 3). S, Cu and Al occupy the most levels, which can be attributed to the association with sulfuric copper mineralization and aluminium bearing minerals such as plagioclase crystals in the quartz monzonitic body (Darrehzar porphyry) (Soltani *et al.* 2014; Ravankhah *et al.* 2009). High concentration of Fe and Mn may have derived from pyrite oxidation and high Fe and S values in water samples probably referred to the presence of acidic mine drainage. The analysis revealed that trace elements such as Al, Fe, Mn and S are significantly enriched in acid water and vary seasonally, increasing from winter to summer in the mine. This situation was also observed in the study implemented by Ferreira da Silva *et al.* (2015). Furthermore, the concentration of the elements (except Mo) in acidic water in the inside of the mine including the surface water lake in the eastern part of the mine (Da23) and the surface water pit lake in the western part of the mine (Da20) were much more than neutral water from the influx and discharging water of the mine. This can arise from the fact that Mo
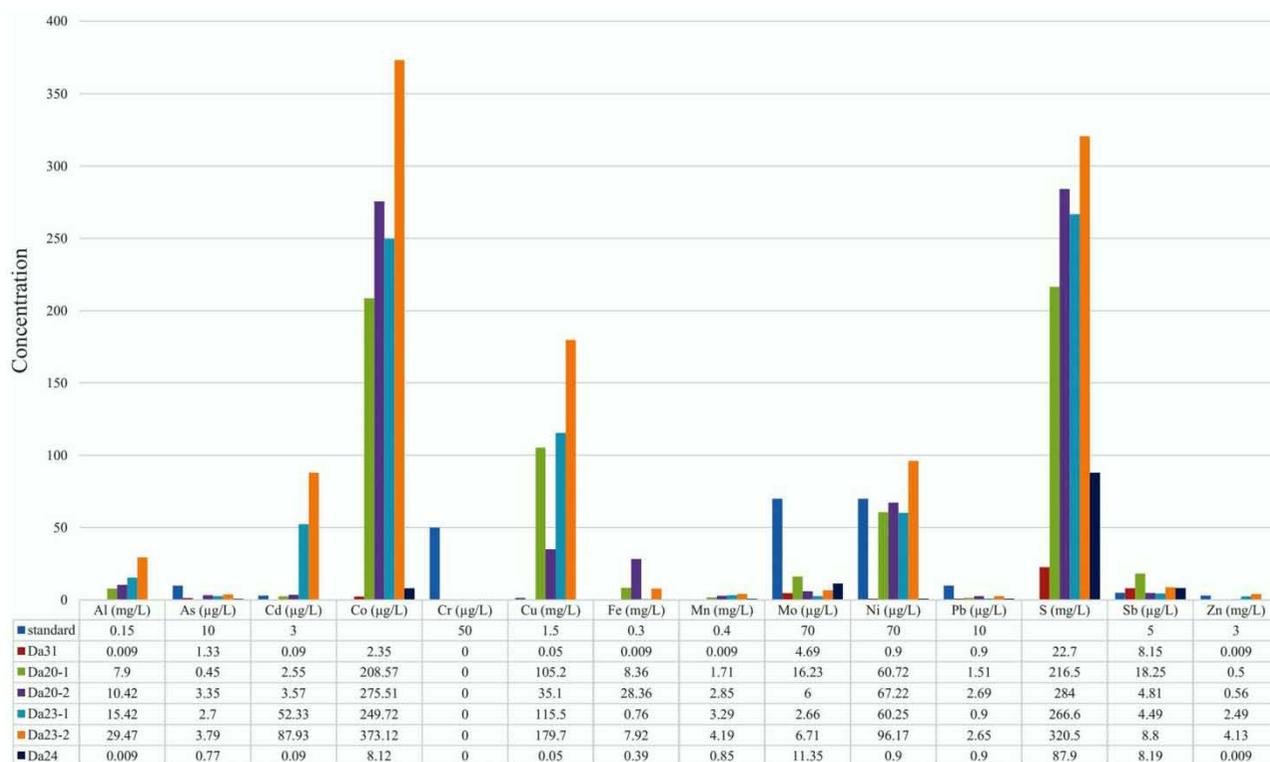

	Al (mg/L)	As (μg/L)	Cd (μg/L)	Co (μg/L)	Cr (μg/L)	Cu (mg/L)	Fe (mg/L)	Mn (mg/L)	Mo (μg/L)	Ni (μg/L)	Pb (μg/L)	S (mg/L)	Sb (μg/L)	Zn (mg/L)
standard	0.15	10	3		50	1.5	0.3	0.4	70	70	10		5	3
Da31	0.009	1.33	0.09	2.35	0	0.05	0.009	0.009	4.69	0.9	0.9	22.7	8.15	0.009
Da20-1	7.9	0.45	2.55	208.57	0	105.2	8.36	1.71	16.23	60.72	1.51	216.5	18.25	0.5
Da20-2	10.42	3.35	3.57	275.51	0	35.1	28.36	2.85	6	67.22	2.69	284	4.81	0.56
Da23-1	15.42	2.7	52.33	249.72	0	115.5	0.76	3.29	2.66	60.25	0.9	266.6	4.49	2.49
Da23-2	29.47	3.79	87.93	373.12	0	179.7	7.92	4.19	6.71	96.17	2.65	320.5	8.8	4.13
Da24	0.009	0.77	0.09	8.12	0	0.05	0.39	0.85	11.35	0.9	0.9	87.9	8.19	0.009

Figure 3 │ Concentration of trace elements and sulfur in the water samples of Darrehzar mine (Da31: surface water river in the mine site (upstream); Da20-1 and Da20-2: surface water pit lake in the western part of the mine; Da23-1 and Da23-2: surface water lake in the eastern part of the mine; Da24: surface water river in the mine site (downstream)).

has a different geochemical behavior in acidic conditions and is insoluble in low pH values (Moor *et al.* 2012; Soltani *et al.* 2014). In addition, higher concentrations of Al, As, Cd, Co, Cu, Mn, S, Ni and Zn were observed in water samples from the surface water lake in the eastern part of the mine. While the highest concentrations of Fe, Mo, Pb and Sb were observed in surface water samples from the pit lake in the western part of the mine especially in the summer (Figure 3). The values of Mn, Co and Ni from the surface water lake (pH = 4.28 in winter and 3.18 in summer) are more than the values for these elements in the surface water pit lake (pH = 3.48 in winter and 2.75 in summer), while the Fe concentration was higher in the surface water pit lake. This can be attributed to the geochemical behavior of these elements so that Fe precipitates at lower
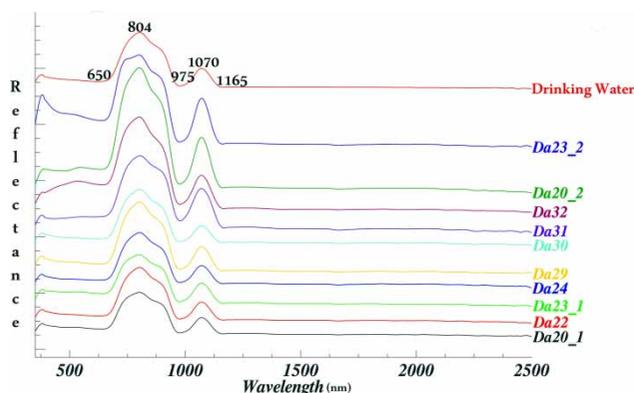
pH relative to Mn, Cr, Co and Ni. It also should be noticed that Al, Cd, Cu, Fe, Mn, Ni, Sb and Zn levels exceeded the defined MCL determined by the World Health Organization (WHO 2011), Codex Standard 108 (1981) and the Institute of Standards and Industrial Research of Iran (ISIRI 2441 2004; ISIRI 1053 2009) (Figure 3). There is no MCL level defined for cadmium (Cd) and sulfur (S) by WHO, Codex Standard and ISIRI for drinking and natural mineral water.

Absorption features

Spectral measurements were carried out for all of the samples as well as drinking water (Figure 4). Results of spectroscopy showed that the water spectra were similar, with negligible differences. Three absorption features at 650, 975 and 1,165 nm and two reflectance peaks at 804 and 1,070 nm can be observed in the water spectra. The absorption features relatively correspond with the results stated in Yamanouchi & Tanaka (1985), which measured and estimated water vapor (H_2O) absorptions in VNIR at 900 and 1,100 nm. In addition, Sullivan *et al.* (2006) stated an absorption feature at 662 nm for water, with temperature dependency.

The magnitude of three absorption features at 650, 975 and 1,165 nm, which were indicated by AF1, AF2 and AF3 respectively, were determined using Equation (1) (Figure 5). Result of absorption feature analysis illustrated that drinking water contains higher values of absorption magnitudes than Darrehzar water samples at all absorption features except the second absorption feature of Da23-2. In addition,

Figure 4 │ Spectra of collected water samples from Darrehzar mine; the first absorption feature (AF1) located in 650 nm, the second absorption feature (AF2) in 975 nm and the third absorption feature (AF3) in 1,165 nm.
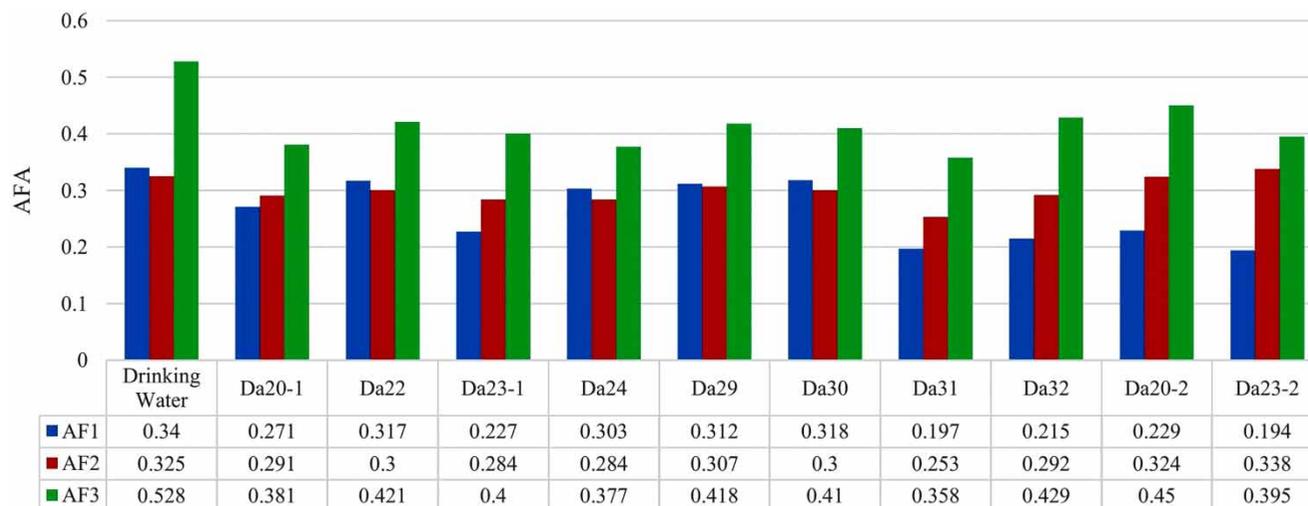

	Drinking Water	Da20-1	Da22	Da23-1	Da24	Da29	Da30	Da31	Da32	Da20-2	Da23-2
■ AF1	0.34	0.271	0.317	0.227	0.303	0.312	0.318	0.197	0.215	0.229	0.194
■ AF2	0.325	0.291	0.3	0.284	0.284	0.307	0.3	0.253	0.292	0.324	0.338
■ AF3	0.528	0.381	0.421	0.4	0.377	0.418	0.41	0.358	0.429	0.45	0.395

Figure 5 │ Result of absorption feature analysis (AFA) in water spectra (Da20-1 and Da20-2: Surface water pit lake in the western part of the mine; Da22: Surface water river in the mine site; Da23-1 and Da23-2: Surface water lake in the eastern part of the mine; Da24: Surface water river in the mine site (downstream); Da29: Surface water river in the mine site; Da30: Surface water river in the mine site; Da31: Surface water river in the mine site (upstream); Da32: groundwater (piezometer well) in the mine).

comparison of the results revealed that the influx water to the mine (Da31) contains the lowest values and this sample had the lowest levels of EC and dissolved metal as well (Figure 5 and Table 2). The amount of absorption magnitude for the third absorption feature for all samples is more than the two other absorption features. The second absorption feature's magnitudes of acidic water (Da20-1, Da20-2, Da23-1 and Da23-2), water with colloids (Da32) and surface water river in the upstream (Da31) are bigger than the first absorption feature's magnitudes, and vice versa for other water samples (Da22, Da24, Da29 and Da30) (Figure 5). The samples with higher EC such as Da20-2, Da23-2 and Da32 presented more differences

between the first and second absorption features. However, it is not accurate for Da30 (high EC and low difference) and Da31 (low EC and high difference). This shows that besides EC, other processes such as the presence of elements and colloids could be influences on the spectral characteristics.

Furthermore, comparison of spectra in Figure 4 showed that the absorption value is reduced in the spectra of acidic water such as Da20 and Da23 and they represent a small reflectance at 548 and 518 nm, respectively (Figure 6(a)). This is probably associated with dissolved particles e.g. Cu-bearing compositions in water samples. Referring to the field studies and the ICP results, the presence of chalcanthite ($CuSO_4.5H_2O$) and high content of Cu and S in
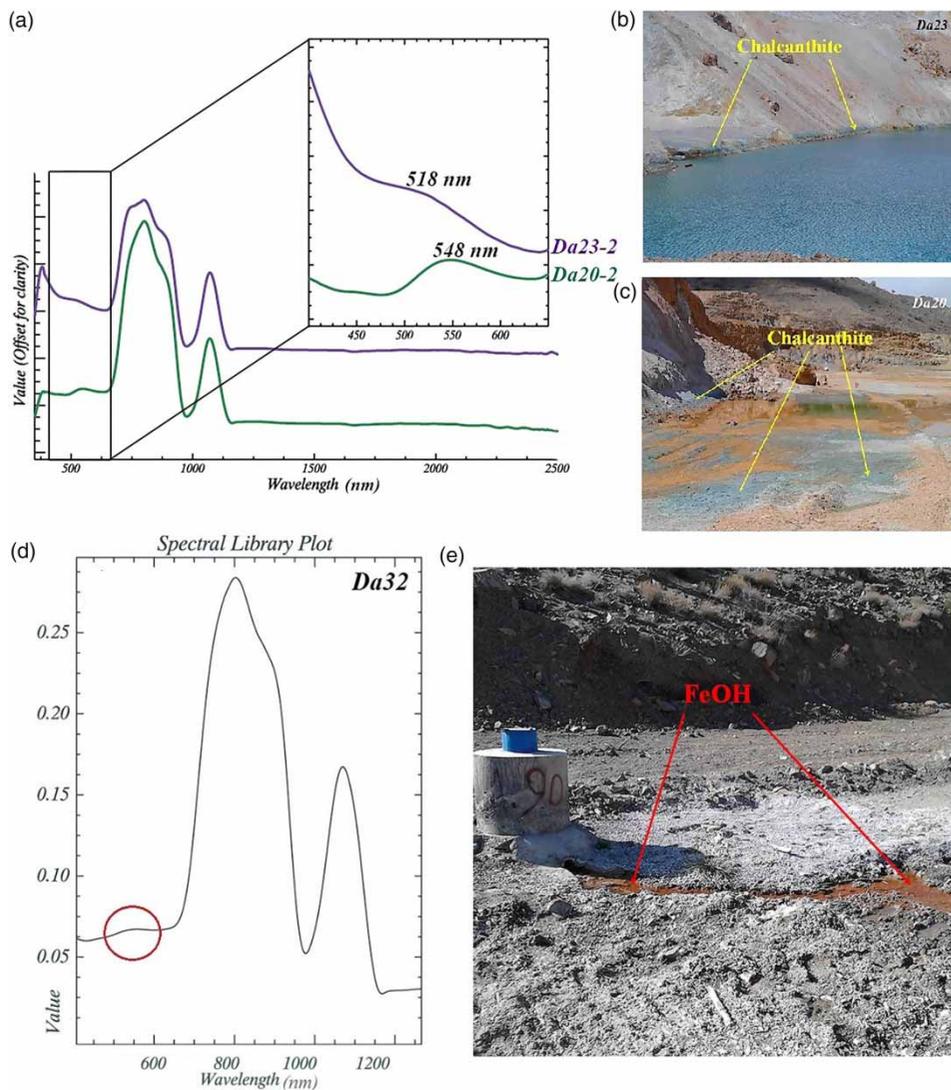

Figure 6 | (a) Spectra of acidic water and their small reflectances at 548 and 518 nm; (b) presence of chalcanthite in surface water lake in the eastern part of the mine (Da23); (c) presence of chalcanthite in surface water pit lake in the western part of the mine (Da20); (d) a broad small reflectance in 546-525 nm of Da32 spectrum (reflectance is located by circle); (e) the piezometer well and FeOH sediments in its stream.

the site of acidic water (surface water lake in the eastern part and surface water pit lake in the western part of the mine), reflecting the fact that $CuSO_4$ particles are in a dissolved state in the water (Figures 3, 6(b) and 6(c)). In addition, a broad small reflectance is seen at 546–525 nm in the spectra of Da32, which have been taken from the piezometer well in the mine (Figure 6(d)). Fe-bearing precipitations downstream from the piezometer well probably reflected the presence of colloids in the water and created the reflectance (Figure 6(e)). Furthermore, the first absorption feature value for acidic water and the water of the piezometer well with colloids was less than the first absorption feature of other samples.

Relationship between absorption features and chemical properties

Table 3 presents the regression (R^2), the equation for calculating regression, and correlation (R) between the magnitudes of absorption features with EC and pH parameters. The first absorption feature correlates positively with pH (0.462) and negatively with EC (-0.425) and vice versa for both the second and third absorption features (Table 3). The second absorption feature displays a significant correlation with pH (-0.599) and EC (0.611) ($p < 0.1$). This region (975 nm) corresponds with the results of Estifanos (2006), which determined the absorption features related to pH and EC in 852–1,036 nm.

Total element concentrations (Al, As, Cd, Co, Cu, Fe, Mn, Mo, Ni, Pb, S, Sb and Zn) show a negative correlation with the first absorption feature and a positive correlation with both the second and the third absorption features (Figure 7). The second absorption feature correlated significantly with total elements (R = 0.822; $p < 0.05$) (Figure 7(b)). Regressions between total elements with pH and EC were also computed

Table 3 │ Regression (R^2) and correlation (R) between absorption features magnitudes and total elements with EC and pH parameters

		Equation	R^2	R
pH	AF1	y = 0.0108x + 0.1948	0.214	0.462
	AF2	y = −0.0064x + 0.3348	0.359	0.599
	AF3	y = −0.0021x + 0.4162	0.028	0.167
EC	AF1	y = −3E-05x + 0.2983	0.181	0.425
	AF2	y = 2E-05x + 0.2713	0.373	0.611
	AF3	y = 2E-05x + 0.3814	0.204	0.451
pH	Total elements	y = −79.59x + 685.1	0.8906	0.943716**
EC	Total elements	y = 0.2403x-52.38	0.8746	0.935201**

**$p < 0.01$.

and show significant relationship (R = 0.94 for pH and R = 0.93 for EC) ($p < 0.01$) (Table 3). It referred that pH and EC parameters can influence trace elements' solution. Thus, dissolved metal concentration rises in water while an increase in EC and a decrease of pH occurs, which was confirmed by Anderson (1994), Tutu *et al.* (2008) and Soltani *et al.* (2014).

There is a significant correlation between the second absorption feature and Co, Mn, Ni, Pb and S ($p < 0.05$) (Figure 8). According to the ICP-MS results, Al, Cu, Mn, S and Zn indicated high concentration in water samples (Figure 3). Gupta (2003) stated that spectral characteristics in the VNIR part of the EM spectrum are dominated by electronic processes in transition metals (e.g. Fe, Mn, Cu, etc.) and the electronic processes in transition Cu occur at 800 nm. This region is situated between the first (650 nm) and second (975 nm) absorption features of the water spectra. In addition, Estifanos (2006) introduced the 996–1,163 nm region as an indicator spectral region to predict Mn in polluted mining areas by the partial least square regression (PLSR) technique. This region is also located between the second and third (1,165 nm) absorption features of the water spectra. Furthermore, the indicator spectral regions at 573–765 nm and 873–1,101 nm were presented for Zn recognition using the PLSR technique (Estifanos 2006). Both regions conform to the first and second absorption features of water spectra as a result; the regression values of these two absorption features are close. Fe, which has a high concentration, shows a significant correlation with the third absorption feature. There are crystal field transitions of ferric iron at 550–650 nm and 750–950 nm as well as at 900–1,100 nm for ferrous iron (Zabcic 2008). The electronic transition of ferrous iron conforms to the third absorption feature (Figure 8).

CONCLUSION

Results of the pH and EC measurements showed that water with low pH, high EC and high concentrations of trace elements and S was located inside the mine and water with high pH, low EC and low concentrations of the elements was situated in the influx and discharging parts of the mine. Moreover, the collected water samples in summer displayed lower pH, higher EC and dissolved metals than water samples of the winter season. Large amounts of copper and sulfur in the water samples could be related to copper mineralization in the phyllic alteration zone. Furthermore, water with low pH, high iron and sulfur concentrations was associated with the phyllic zone and this

(a) $y = -7E\text{-}05x + 0.257$

$R^2 = 0.101$ $R = 0.317$

(b) $y = 0.0001x + 0.2584$

$R^2 = 0.676$ $R = 0.822$ ✳

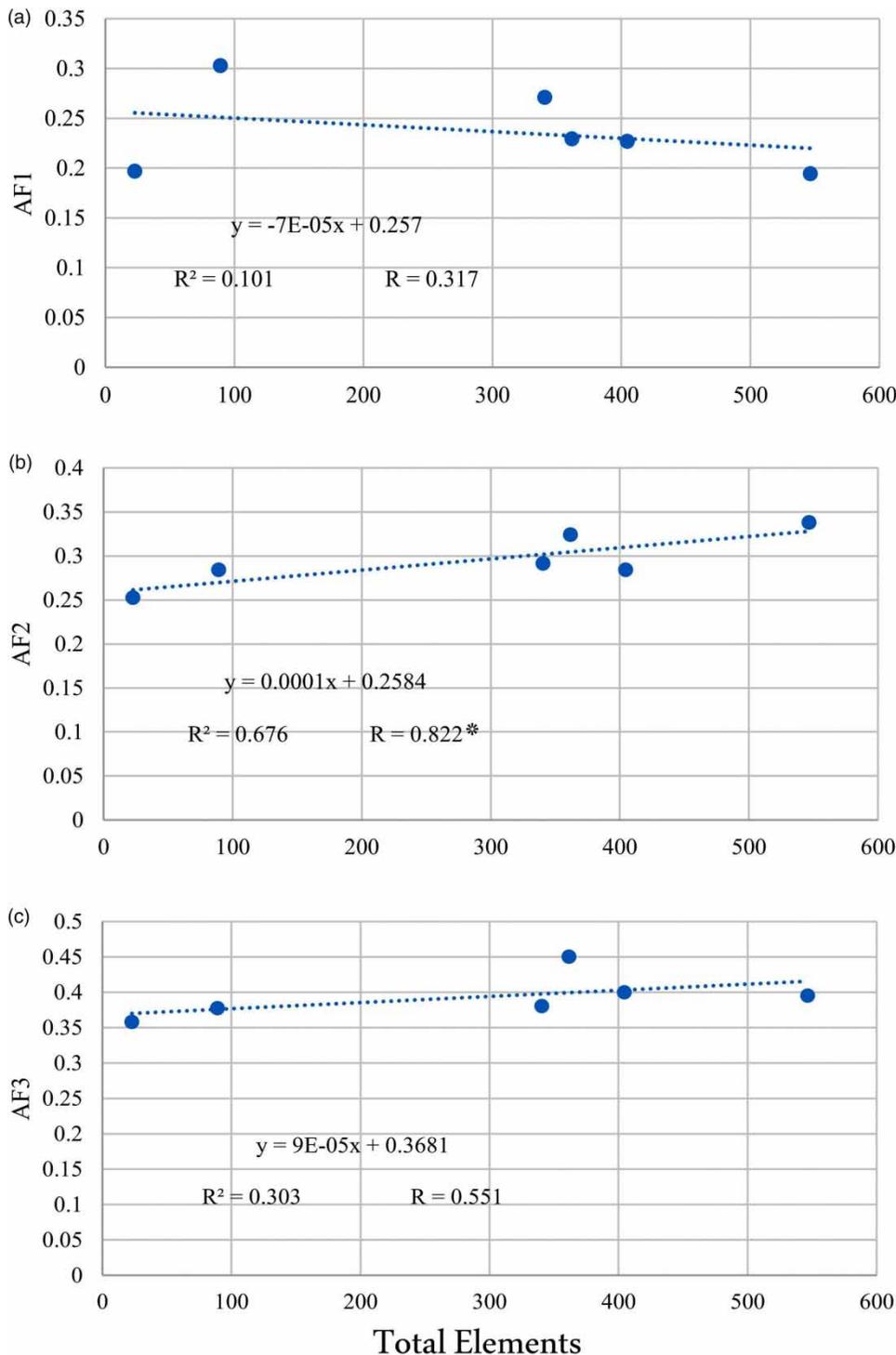(c) $y = 9E\text{-}05x + 0.3681$

$R^2 = 0.303$ $R = 0.551$

Figure 7 | (a) The relationship between the first absorption feature with total elements; (b) the relationship between the second absorption feature with total elements; (c) the relationship between the third absorption feature with total elements (*$p < 0.05$).

condition normally happens due to the oxidation of pyrite and producing acid mine drainage. Results of spectroscopic studies presented similar spectra for water samples that contain three absorption features in the visible-near infrared region. The second absorption feature (AF2) magnitude correlated significantly with total elements (0.822) ($p < 0.05$). The close correlation between the AF2 magnitude with S (0.854), Pb (0.914), Ni (0.836), Mn (0.834), Co (0.848)
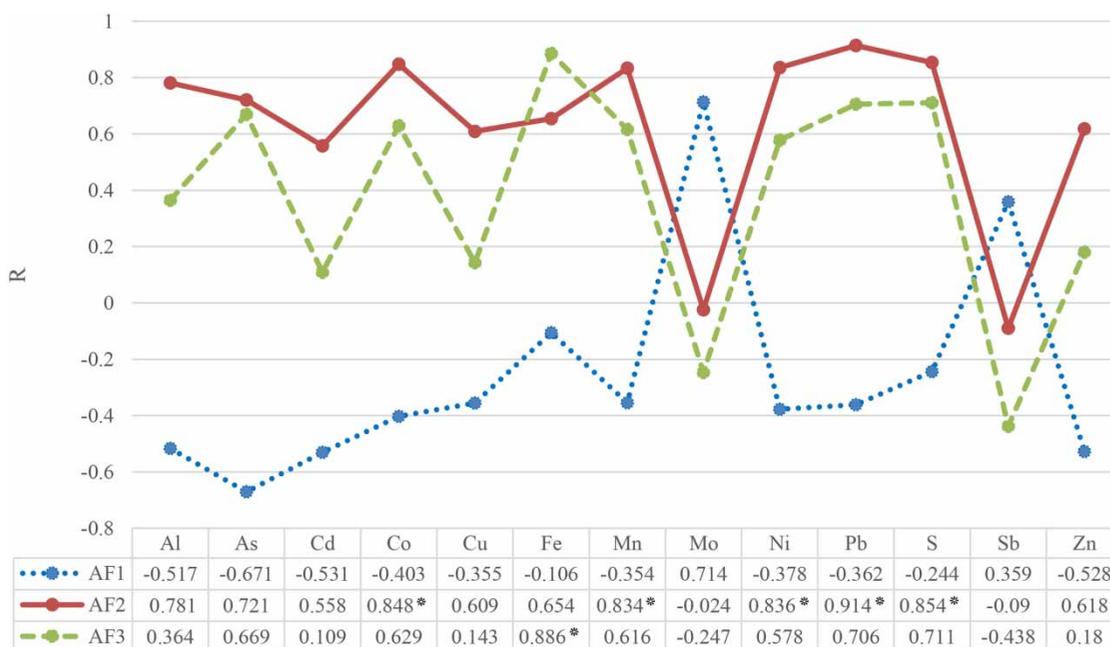
	Al	As	Cd	Co	Cu	Fe	Mn	Mo	Ni	Pb	S	Sb	Zn
AF1	-0.517	-0.671	-0.531	-0.403	-0.355	-0.106	-0.354	0.714	-0.378	-0.362	-0.244	0.359	-0.528
AF2	0.781	0.721	0.558	0.848*	0.609	0.654	0.834*	-0.024	0.836*	0.914*	0.854*	-0.09	0.618
AF3	0.364	0.669	0.109	0.629	0.143	0.886*	0.616	-0.247	0.578	0.706	0.711	-0.438	0.18

Figure 8 | The correlation (R) between the elements concentrations with absorption feature magnitudes of water spectra (*$p < 0.05$.).

concentrations and third absorption feature (AF3) magnitude with Fe (0.886) concentration showed that the magnitude of the absorption feature increases when the concentration of elements increases in water. However, changes in the magnitude of the absorption feature are negligible compared to changes in the elements. Although the results show that trace elements and S concentrations, EC and pH can affect the spectral properties of water and there is a correlation between them, much effort remains to be made in other areas and more samples to verify the accurate determination and investigation of the effects of colloidal particles (e.g. FeOH and $CuSO_4$).

ACKNOWLEDGEMENTS

REFERENCES

Anderson, J. 1994 Spectral characterization of acid-mine and neutral-drainage bacterial precipitates and their relationship to water quality in a Piedmont watershed. *Virginia Journal of Science* **45**, 175–186.

Anderson, J. & Robbins, E. 1998 Spectral reflectance and detection of iron-oxide precipitates associated with acidic mine drainage. *Photogrammetric Engineering & Remote Sensing* **64**, 1201–1208.

Blahwar, B. 2010 *Identification of the Extent of Artisanal Coal Mining and Related Acid Mine Water Hazards Using Remote Sensing and Field Sampling A Case Study in Jaintia Hills of North-Eastern India*. MSc dissertation, International Institute for Geo-information Science and Earth Observation, Enschede, The Netherlands and the Indian Institute of Remote Sensing, Dehradun, India.

Buiteveld, H., Hakvoort, J. H. M. & Donze, M. 1994 The optical properties of pure water. *SPIE* **2258** (Ocean Optics XII), 174–183.

Choe, E., Meer, F., Ruitenbeek, F., Werff, H., Smeth, B. & Kim, K. W. 2008 Mapping of heavy metal pollution in stream sediments using combined geochemistry, field spectroscopy, and hyperspectral remote sensing: a case study of the Rodalquilar mining area, SE Spain. *Remote Sensing of Environment* **112**, 3222–3233.

Codex Standard 108. 1981 *CODEX Standard for Natural Mineral Waters*.

Costello, C. 2003 *Acid Mine Drainage: Innovative Treatment Technologies*. National Network of Environmental Management Studies Fellow for U.S. Environmental Protection Agency, Washington.

Estifanos, S. 2006 *Spectral Indicators for Assessing Pollution in the Epithermal Gold Mining Area of Rodalquilar, SE Spain*. MS dissertation, International Institute for Geo-information Science and Earth Observation, Enschede, The Netherlands.

Ferreira da Silva, E., Durães, N., Reis, P., Patinha, C., Matos, J. & Costa, M. R. 2015 An integrative assessment of environmental

degradation of Caveira abandoned mine area (Southern Portugal). *Journal of Geochemical Exploration* **159**, 33–47.

Geological Survey of Iran (GSI) 1973 *Exploration for ore Deposit in Kerman Region*. Geological Survey of Iran Report Y/53, Tehran.

Gupta, R. P. 2003 *Remote Sensing Geology. Second Edition*. Springer-Verlag Berlin Heidelberg, New York.

Gyuris, P., Tote, C., Reusen, I., Delalieux, S. & Kolodyazhnyy, O. 2010 *WP4-Satellite Remote Sensing, Deliverable D4.1, Report on the Limitations and Potentials of Satellite EO Data*. GEONARDO Environmental Technologies Ltd, Hungary.

Hosseinjani Zadeh, M., Tangestani, M. H., Velasco Roldan, F. & Yusta, I. 2014 Spectral characteristics of minerals in alteration zones associated with porphyry copper deposits in the middle part of Kerman copper belt, SE Iran. *Ore Geology Reviews* **62**, 191–198.

ISIRI 1053 2009 *Drinking Water-Physical and Chemical Specifications*, 5th revision edn. Institute of Standards and Industrial Research of Iran, Tehran, Iran.

ISIRI 2441 2004 *Natural Mineral Water – Specifications*, 1st edn. Institute of Standards and Industrial Research of Iran, Tehran, Iran.

Khalili, R., Anvari, S. & Honarmand, M. 2015 Combination of Biochemical and Hyperspectral Remote Sensing Methods for Detection of Heavy Metal Pollutions in Eucalyptus Leaves (Case Study: The City of Bam). In: *International Conference on Sensors & Models in Remote Sensing & Photogrammetry, Kish Island, Iran*.

Li, Q., Yang, F., Zhang, B., Zhang, X. & Zhou, G. 2008 Biogeochemistry responses and spectral characteristics of Rhus Chinensis Mill under heavy metal contamination stress. *Journal of Remote Sensing* **12** (2), 284–290.

Moor, F., Soltani, N., Keshavarzi, B., Esmaeel Zadeh, A. & Karimi, M. 2012 Environmental geochemistry of water, soil, and sediments in Darrehzar copper deposit (Kerman). *Journal of Advanced Applied Geology* **3**, 29–37.

Nateghi, A. & Hezarkhani, A. 2013 Fluid inclusion evidence for hydrothermal fluid evolution in the Darreh-Zar porphyry copper deposit, Iran. *Journal of Asian Earth Sciences* **73**, 240–251.

Ranjbar, H., Roonwal, G. S., Ravindran, K. V. & Babar, S. 2000 Synergetic use of remote sensing and geophysical data for exploration of porphyry copper deposits, using GIS. *Journal of the Indian Society of Remote Sensing* **28** (2&3), 205–212.

Ravankhah, A., Moaiyad, M., Amini, S. & Hossein Zadeh, G. 2009 Discussion of geology, petrology, economic geology and alteration zones in Darrehzar porphyry copper deposit (South West of Kerman). *Journal of Geological Survey of Iran* **12**, 63–75.

Rueda, C. A. & Wrona, A. F. 2003 *Spectral Analysis and Management System, User's Manual*, Version 2.0 edn. University of California, Davis, California.

Shi, X., Aspandiar, M. & Oldmeadow, D. 2014 Reflectance spectral characterization and mineralogy of acid sulphate soil in subsurface using hyperspectral data. *International Journal of Sediment Research* **29**, 149–158.

Soltani, N., Moore, F., Keshavarzi, B. & Sharifi, R. 2014 Geochemistry of trace metals and rare earth elements in stream water, stream sediments and acid mine drainage from Darrehzar copper mine, Kerman, Iran. *Water Quality Exposure and Health* **6**, 97–114.

Sullivan, J. M., Twardowski, M. S., Zaneveld, J. R., Moore, C. M., Barnard, A. H., Donaghay, P. L. & Rhoades, B. 2006 The hyperspectral temperature and salt dependencies of absorption by water and heavy water in the 400–750 nm spectral range. *Applied Optics* **45**, 5294–5309.

Tutu, H., McCarthy, T. S. & Cukrowska, E. 2008 The chemical characteristics of acid mine drainage with particular reference to sources, distribution and remediation: the Witwatersrand Basin, South Africa as a case study. *Applied Geochemistry* **23**, 3666–3684.

van der Meer, F. D. & de Jong, S. M. 2006 *Imaging Spectrometry, Basic Principles and Prospective Applications*. Springer, Dordrecht, The Netherlands.

Wang, L. 2008 *Measuring Optical Absorption Coefficient of Pure Water in UV Using the Integrating Cavity Absorption Meter*. PhD thesis, Texas A&M University.

WHO 2011 *Guidelines for Drinking-Water Quality*, 4th edn. World Health Organization, Geneva, Switzerland.

Yamanouchi, T. & Tanaka, M. 1985 Absorption properties of the near-infrared water vapor bands. *Journal of Quantitative Spectroscopy and Radiative Transfer* **34** (6), 463–472.

Zabcic, N. 2008 *Derivation of Surface pH-Values Based on Mineral Abundances Over Pyrite Mining Areas with Airborne Hyperspectral Data (Hymap) of Sotiel-Migollas Mine Complex, Spain*. MS dissertation, University of Alberta, Edmonton.